JOURNAL OF PLANKTON RESEARCH | VOLUME 23 | NUMBER 4 | PAGES 333–352 | 2001

Antarctic phytoplankton assemblages in the marginal ice zone of the northwestern Weddell Sea

SUNG-HO KANG, JAE-SHIN KANG, SANGHOON LEE, KYUNG HO CHUNG, DONGSEON KIM AND MYUNG GIL PARK[1,2]

POLAR SCIENCES LABORATORY, KOREA OCEAN RESEARCH AND DEVELOPMENT INSTITUTE (KORDI), ANSAN PO BOX 29, SEOUL 425-600 AND [1]DEPARTMENT OF OCEANOGRAPHY, COLLEGE OF NATURAL SCIENCES, SEOUL NATIONAL UNIVERSITY, SEOUL 151-742, REPUBLIC OF KOREA

[2]PRESENT ADDRESS: SMITHSONIAN ENVIRONMENTAL RESEARCH CENTER, PO BOX 28, EDGEWATER, MD 21037, USA

The waters around the northern tip of the Antarctic Peninsula show complex patterns of water circulation due to mixing of diverse water masses. Physicochemical properties of the different water types should affect the distribution, biomass and species composition of the phytoplankton assemblages. We examined these features in the marginal ice zone (MIZ) of the northwestern Weddell Sea. Areas with the higher biomass were located in the Weddell Sea MIZ where the surface waters were relatively stable due to the sea-ice melting. In these waters, the colonial stage of Phaeocystis antarctica and micro-sized chain-forming diatoms accounted for 70% of the total phytoplankton carbon. Waters in the Bransfield Strait region, in contrast, were characterized by a dominance of nanoflagellates, which accounted for 80% of the total phytoplankton carbon. Our observations support the hypothesis that the species composition of phytoplankton communities is a function of the different water mass, reflecting the physical conditions of the upper water column, particularly its stability.

INTRODUCTION

The Weddell Sea marginal ice zone (MIZ) is a region of high phytoplankton biomass and productivity (Garrison *et al.*, 1987, 1993; Fryxell and Kendrick, 1988; Smith and Nelson, 1990; Cota *et al.*, 1992; Kang and Fryxell, 1993; Kang *et al.*, 1995; Park *et al.*, 1999). In contrast, open waters of the Bransfield Strait region, well away from the melting of sea ice, are characterized by low phytoplankton biomass and primary production due to weak vertical stratification and deep vertical mixing which limits available irradiance [e.g. (Holm-Hansen and Mitchell, 1991; Lancelot *et al.*, 1993; Kang and Lee, 1995)].

We have tried to examine the water mass structure to test the hypothesis that the distribution of phytoplankton at the species level varies primarily with different water masses. The physical structure of the surveyed area can be linked to biological and chemical variables and aid biophysical interpretation (Pollard *et al.*, 1995). An essential prerequisite for phytoplankton bloom development is vertical stratification to confine phytoplankton to the euphotic zone [e.g. (Sverdrup, 1953; Mitchell and Holm-Hansen, 1991)]. Thus, the blooms have been observed in the MIZ where a shallow layer of relatively fresh water from melting ice stabilizes the surface layer (Smith and Nelson, 1986). Such mesoscale blooms have a significant impact on the annual productivity, trophic dynamics and biogeochemical cycles of the entire Southern Ocean (Arrigo *et al.*, 1998).

The MIZ of the northwestern Weddell Sea and the eastern Bransfield Strait region was chosen as our study area. It includes the coastal shelf, the continental shelf break, island shelves, and deep waters of the Bransfield Strait, Drake Passage and Weddell Sea. It is characterized by complex physical circulation and the presence of several different water masses and frontal structures (Capella *et al.*, 1992; Hofmann *et al.*, 1996). The study area is one of the few areas in the Southern Ocean where the open ocean, seasonal sea ice and permanent pack ice occur close to each other, reflecting the complex patterns of water circulation and the annual cycle of sea-ice formation and ablation (Capella *et al.*, 1992; Hofmann *et al.*, 1996; Hewitt, 1997). Preliminary studies of the phytoplankton in the study area showed that the initiation, continuation and demise of blooms are controlled largely by the physical water column properties (Park *et al.*, 1999).

The objectives of this study were: (i) to measure the size and biomass distribution of key phytoplankton species;

(ii) to evaluate phytoplankton species composition and biomass across the ice-edge zones and open waters both horizontally and vertically; (iii) to determine the magnitude and extent of the MIZ phytoplankton bloom; and (iv) to understand the dynamics of the phytoplankton bloom in the MIZ.

METHOD

Sample collection

Phytoplankton assemblages in the northwestern Weddell Sea and the eastern Bransfield Strait region were sampled from 4 to 14 January 1995 aboard RV 'Yuzhmorgeologiya'. Data were acquired at 38 stations along the north–south transects extending from the Weddell Sea to Drake Passage (Figure 1). The transects lie from the coastal shelf to the deep waters of Drake Passage, crossing the continental shelf break and slope, basin and island shelves. The northern portion of the study area was located in the deep waters (>3000 m) of Drake Passage. The southern portion of the study area was located in the Weddell Sea MIZ.

Salinity and temperature were measured with a Mark V CTD profiler (General Oceanics, Inc.). Water samples were obtained with a CTD/rosette unit at seven discrete depths (0, 10, 20, 30, 50, 75 and 100 m) in 5 l PVC Niskin bottles. Aliquots of 125 ml were preserved with glutaraldehyde (final concentration 1%). Phytoplankton samples were also collected in nets (20 μm mesh) and preserved with glutaraldehyde (final concentration 2%); these samples were for the analysis of rare species.

Sample volumes of 50–100 ml were filtered through Gelman GN-6 Metricel filters (0.45 μm pore size, 25 mm diameter). The filters were mounted on microscope slides with water-soluble embedding medium [2-hydroxypropyl methacrylate (HPMA)] on board RV 'Yuzhmorgeologiya' (Crumpton, 1987). The slides were used to estimate cell concentration and biomass. The HPMA mounting technique was first described by Crumpton (Crumpton, 1987)

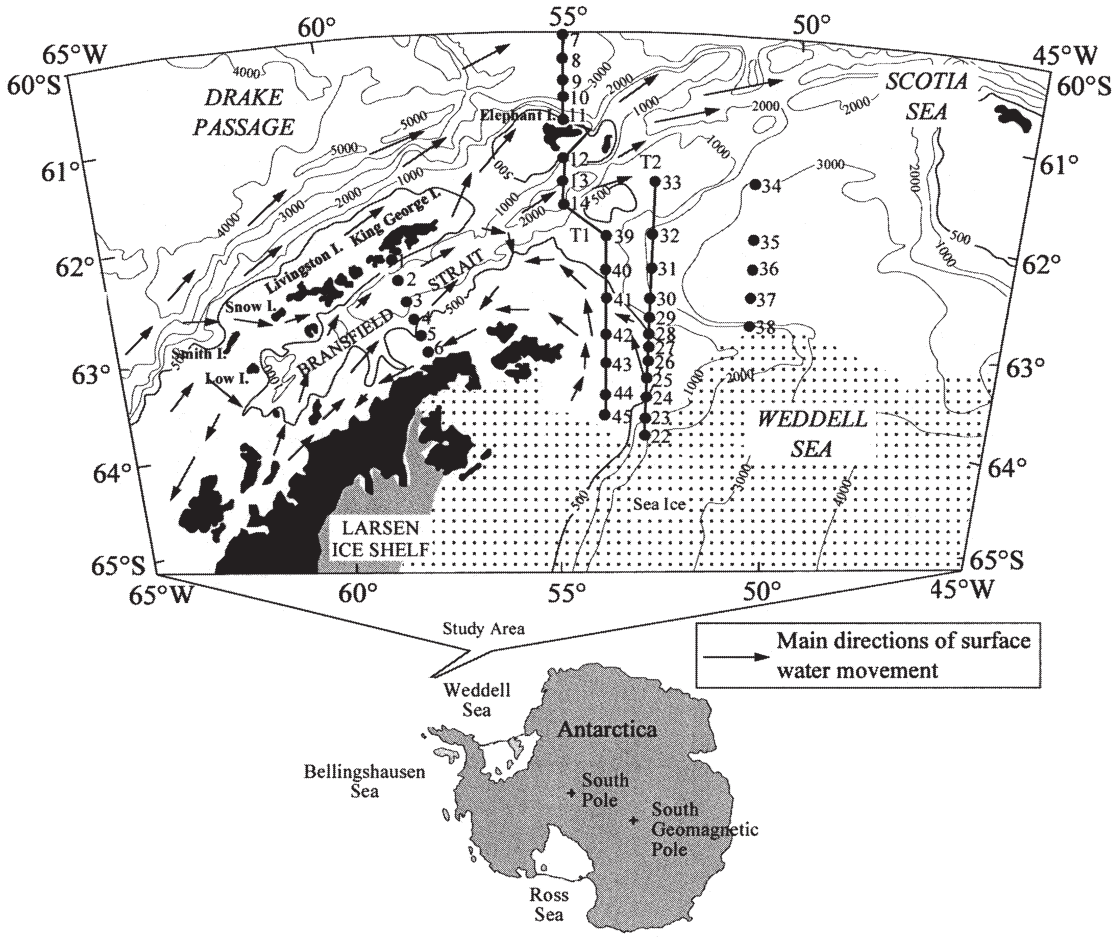

Fig. 1. Location of the sampling area and the major water masses. The main directions of surface water movement are shown by the arrows [after (Hofmann *et al.*, 1992)]. Station locations during the 1995 KARP cruise, which were occupied from 4 to 14 January 1995.

and has been used for quantitative analysis of the Antarctic phytoplankton (Kang and Fryxell, 1991, 1992; Kang *et al.*, 1993a,b, 1995; Kang and Lee, 1995; Bidigare *et al.*, 1996).

Cell count, biovolume and biomass of phytoplankton

The HPMA slides were examined within 1 year of collection using light microscopy (LM) and epifluorescence microscopy (EFM). Most of the pico- (cells <2 μm) and nanophytoplankton (cells 2–20 μm) were enumerated using EFM with blue light excitation using a Zeiss Axiophot microscope equipped for epifluorescence (Zeiss filter set 48 77 09, reflector 510 nm, excitation 450–490 nm, barrier filter at 520 nm, 50 W mercury light source). Microphytoplankton (cells >20 μm) were enumerated using LM. Magnification was chosen according to cell size: ×1000 for cells <20 μm, ×400 for cells ranging between 20 and 60 μm, and ×100 or ×200 for larger cells. Cells were counted in random fields until 300–500 had been observed in total.

Conversions from cell counts to cell concentrations were carried out as described previously by Kang and Fryxell (Kang and Fryxell, 1991) and Kang *et al.* (Kang *et al.*, 1993a). Cell dimensions of dominating phytoplankton species were measured to the nearest 1 μm for subsequent estimations of biovolume using appropriate geometrical shapes (Table I). The carbon (C) biomass was estimated from the cell biovolume with the modified Strathmann equations [equations (7) and (8) in Smayda (Smayda, 1978)]. For autotrophic flagellates, the relationship $\log_{10}$ C (pg) = 0.94 $\log_{10}$ [cell volume (μm^3)] – 0.60 was used, and for diatoms, $\log_{10}$ C (pg) = 0.76 $\log_{10}$ [cell volume (μm^3)] – 0.352.

Inorganic nutrients

For analysis of nitrate and silicate, 200 ml of seawater sample were filtered through Whatman GF/F glass fiber filters, and the filtrates were stored frozen in acid-cleaned polyethylene bottles at –45°C. The samples were kept frozen with dry ice during transport to the Korea Ocean Research and Development Institute (KORDI). The nutrient concentrations were determined with a Technicon Autoanalyser II by the method described in Grasshoff *et al.* (Grasshoff *et al.*, 1983).

Chlorophyll *a* analysis

Discrete water samples for the determination of chlorophyll *a* (Chl *a*) were filtered onto Whatman GF/F glass fiber filters. Concentrations of Chl *a* were determined on a Model 10-005R Turner Designs fluorometer, after 24 h extraction in 90% acetone at 4°C without grinding (Parsons *et al.*, 1984).

Autotrophic C to Chl *a* ratio (C:Chl *a*)

Carbon to chlorophyll *a* ratios for the phytoplankton community were obtained by dividing total autotrophic C estimated from the microscope data by the Chl *a* concentrations (mean concentrations of C:Chl *a*).

Statistical analysis

The computer programs KaleidaGraph and SYSTAT for Macintosh were used for the statistical treatment of the C biomass and environmental data, correlation and cluster analyses. Statistical analysis yielded Pearson's correlation coefficient (r), which is the linear association between physicochemical variables and phytoplankton species that are normally distributed. The spatial arrangement of phytoplankton communities was examined by applying a cluster analysis of the phytoplankton C data with the Euclidean distance as similarity index. To normalize distributions and eliminate zero values, the C biomass values were transformed using the log factor: $\log_{10}(x + 1)$. Carbon biomass values of dominant phytoplankton species integrated in the upper 100 m (mg C m^{-2}) were used as variables, and stations were grouped by an average-linkage clustering method. We reduced the number of variables by selecting the dominant phytoplankton species in order to facilitate the interpretation of results and avoid the problem of including rare species, as discussed by Gould (Gould, 1987).

RESULTS

Sea-ice effect on hydrography

The bottom depths from the Bransfield Strait onto the continental shelf of the northeastern fringe of the Antarctic Peninsula exceed 1500 m in the basins of Bransfield Strait and shoal to <500 m at the southern stations in the Weddell Sea (Figure 1). The southern portion of the study region is typically covered with multi-year pack ice throughout the year, whereas the Bransfield Strait portion is ice free in summer (approximately December–April) and partially to completely ice covered for the remainder of the year (Zwally *et al.*, 1983; Stammerjohn and Smith, 1996; Hewitt, 1997). The oceanographic characteristics of the waters around the study area are partly due to (i) the confluence of different waters from the Bellingshausen Sea, Bransfield Strait and Weddell Sea, each of which is different in regard to temperature, nutrient content and salinity, and (ii) variable seasonal ice cover, which introduces variable amounts of fresh water into the water column.

During the austral summer cruise in the northwestern Weddell Sea MIZ, the sea-ice melting created density (σ_t) gradients that promote water column stability and

Table I: Composition of phytoplankton assemblages in the water column of the Bransfield Strait region and the ice edge zone of the Weddell Sea

Species	Trophic mode	Sh	L (µm)	W (µm)	D (µm)	B (µm)	Vol (µm^3)	Cell carbon (pg C cell^{-1})
Diatoms								
Actinocyclus actinochilus (Ehr.) Simonsen	A	C			46.7	20	34 184	1241
Actinocyclus spiritus Watkins	A	C			33.5	22.8	20 052	827
Azpeitia tabularis (Grun.) Fryxell & Sims	A	C			29.3	20	13 451	611
Banquisia belgicae (V. H.) Paddock	A	R	100	20.2	20		40 480	1411
Chaetoceros bulbosum (atlanticum-phase)	A	R	22	10	10		2200	154
Chaetoceros bulbosum (bulbosum-phase)	A	R	33.4	15	15		7515	392
Chaetoceros concavicornis Mangin	A	R	22.5	20	20		9000	450
Chaetoceros criophilum Castracane	A	R	23.4	20	20		9360	464
Chaetoceros dichaeta Ehrenberg	A	R	15	10.2	10		1530	117
Chaetoceros flexuosum Mangin	A	R	15	14.7	14.5		3197	205
Chaetoceros neglectum Karsten	A	R	8	6	5		240	29
Chaetoceros pelagicus Cleve	A	R	16.5	10.5	10		1733	129
Chaetoceros resting spores	A	R	6	5	5		150	20
Chaetoceros socialis Lauder	A	R	8	6.5	6.3		328	36
Chaetoceros spp.	A	R	6	5	5		150	20
Corethron criophilum Castracane	A	C			20	132.8	41 720	1444
Coscinodiscus oculoides Karsten	A	C			179	121.7	3 063 077	37 799
Coscinodiscus spp.	A	C			179	117.7	2 962 543	36 852
Cylindrotheca closterium (Her.) Reimann et Lewin	A	PS	50	3.2		3.2	268	31
Eucampica antarctica var. *recta* (Mangin) Fryxell et Prasad	A	R	80.5	32	24.9		64 014	1999
Fragilariopsis curta (V.H.) Hustedt	A	R	23.3	5.5	5		641	60
Fragilariopsis cylindrus (Grun.) Krieger	A	R	17	2.7	2.6		119	17
Fragilariopsis kerguelensis (O'Meara) Hustedt	A	R	29.5	8	8		1888	137
Fragilariopsis linearis (Castracane) Hasle	A	R	54	8	9		3888	238
Fragilariopsis obliquecostata (V.H.) Hasle	A	R	81	9	9		6561	354
Fragilariopsis pseudonana Hasle	A	R	9	5	5		225	27
Fragilariopsis rhombica Hasle	A	R	13	9	9		1053	88
Fragilariopsis ritscheri (Hustedt) Hasle	A	R	49	9	9		3969	242
Fragilariopsis separanda (Hustedt) Hasle	A	R	30	10	10		3000	195
Fragilariopsis sublinearis Hasle	A	R	56	6	6		2016	144
Fragilariopsis vanheurckii (M. Per.) Hasle	A	R	56.3	5	5		1408	110
Fragilariopsis '*nana*' (<20 µm)	A	R	17	2.7	2.6		119	17
Fragilariopsis spp. (girdle 20–40 µm)	A	R	23.3	4	4		373	40
Fragilariopsis spp. (girdle 40–60 µm)	A	R	50	6	5.9		1766	130.5
Fragilariopsis spp. (girdle >60 µm)	A	R	81	7.55	7.5		4587	270
Haslea sp.	A	PS	110	10		9.5	5489	309
Manguinea fusiformis (Manguin) Paddock	A	PS	83.3	9.8		8.5	3633	226
Manguinea rigida (M. Per.,) Paddock	A	R	125	27.5	27		92 813	2651
Navicula glaciei Van Heurck	A	R	7.5	3.3	3		4745	277
Navicula sp.	A	R	55.5	9.5	9		74	12
Nitzschia lecointei Van Heurck	A	PS	49	4		4	411	43
Nitzschia neglecta Hustedt	A	R	52.5	5.5	5		1444	112
Odontella weissflogii (Janisch) Grunow	A	R	83.3	59	22.8		112 153	3061

Table I: continued

Species	Trophic mode	Sh	L (μm)	W (μm)	D (μm)	B (μm)	Vol (μm^3)	Cell carbon (pg C $cell^{-1}$)
Porosira glacialis Jorgensen	A	C			41.5	23.3	31 449	1165
Porosira pseudodenticulata (Hustedt) Jouse	A	C			64.5	30	98 024	2763
Proboscia alata (Brightwell) Sundström	A	C			14	265.6	40 886	1422
Proboscia inermi Castracane	A	C			12	263.7	29 824	1119
Proboscia truncata Karsten	A	C			30	165.4	116 914	3159
Pseudo-nitzschia heimii Manguin	A	PS	80	4.8		4.8	965	82
Pseudo-nitzschia liniola Cleve/*turgiduloides* Hasle	A	PS	140	2.7		2.7	534	53
Pseudo-nitzschia prolongatoides Hasle	A	PS	19.5	2		2	41	7.5
Pseudo-nitzschia subcurvata (Hasle) Fryxell	A	PS	87	2.5		2.5	285	33
Rhizosolenia antennata f. *semispina* Sundström	A	C			25.5	803	410 096	8200
Stellarima microtrias (Her.) Hassle et Sims	A	C			65.1	43.9	145 943	3739
Thalassiosira antarctica Comber	A	C			29.3	19.9	13 418	610
Thalassiosira frenguelliopsis Fryxell & Johansen	A	C			19	12.9	3663	227
Thalassiosira gracilis (Karsten) Hustedt	A	C			17	11.6	2633	177
Thalassiosira gracilis var. *expecta* (Van Land.) Fryxell	A	C			35.5	24.1	23 854	944
Thalassiosira gravida Cleve	A	C			22	15	5702	318
Thalassiosira lentiginosa (Jan.) Fryxell	A	C			55	37.4	88 856	2564
Thalassiosira ritscheri (Hustedt) Hasle	A	C			55.3	37.6	90 308	2596
Thalassiosira trifulta Fryxell	A	C			23	15.6	6481	351
Thalassiosira tumida (Jan.) Fryxell	A	C			55.6	37.8	91 776	2628
Thalassiosira spp. (< 20 μm)	A	C			18	11.7	2977	194
Thalassiosira spp. (>20 μm)	A	C			46	30.4	50 522	1670
Trichotoxon reinboldii (V.H.) Reid et Round	A	R	909	7.45	7.45		50 452	1668
Flagellates								
Bodo spp.	H	S			7		180	33
Choanoflagellates (< 10 μm)	H	PS	8	3	2	3	38	7.6
Choanoflagellates (> 10 μm)	H	PS	13.9	2.7		2.7	53	10.5
Ciliates	H	PS	31.5	20		20	6591	977
Cryptomonas spp.	A	CO	14	8.3	7.8	8.3	223	40
Dictyocha speculum Ehrenberg	A	S			24.5		7700	400
Gymnodinium spp. (<20 μm)	A	PS	16.1	8.1	6	8	546	94
Gymnodinium spp. (> 20 μm)	H	PS	28	10	10	9.6	1407	229
Gyrodinium spp.	H	PS	71.1	24.3		21.2	19 155	2663
Mantoniella spp.	A	S			4.7		54	11
Parvicorbucula socialis (Meunier) Deflandre	H	PS	8	2.8		2.8	33	7
Phaeocystis antarctica Karsten (colony)	A	S			5.6		92	18
Phaeocystis antarctica (motile)	A	S			3.3		19	4
Prymnesium/Chrysochromulina spp.	A	S			6		113	21
Pyramimonas spp.	A	S			7.6		225	41
Siliceous cysts	A	S			3.5		22	4.7
Undetermined flagellate spp. (4–5 μm)	A	S			4.9		62	12
Undetermined heterotrophic dinoflagellates	H	PS	28	10	10	9.6	1407	229
Undetermined picoflagellates	A	S			1.8		3	0.7

Average cell volume and cell C were determined microscopically. See Method for details of the analysis. D, diameter; L, length; W, width; B, breadth or height; Vol, cell volume. Shapes (Sh) were used to estimate volume from linear dimensions: R, rectangular; C, cylinder; S, sphere; CO, cone; PS, prolate spheroid. Trophic mode: A, autotrophic mode; H, heterotrophic mode.

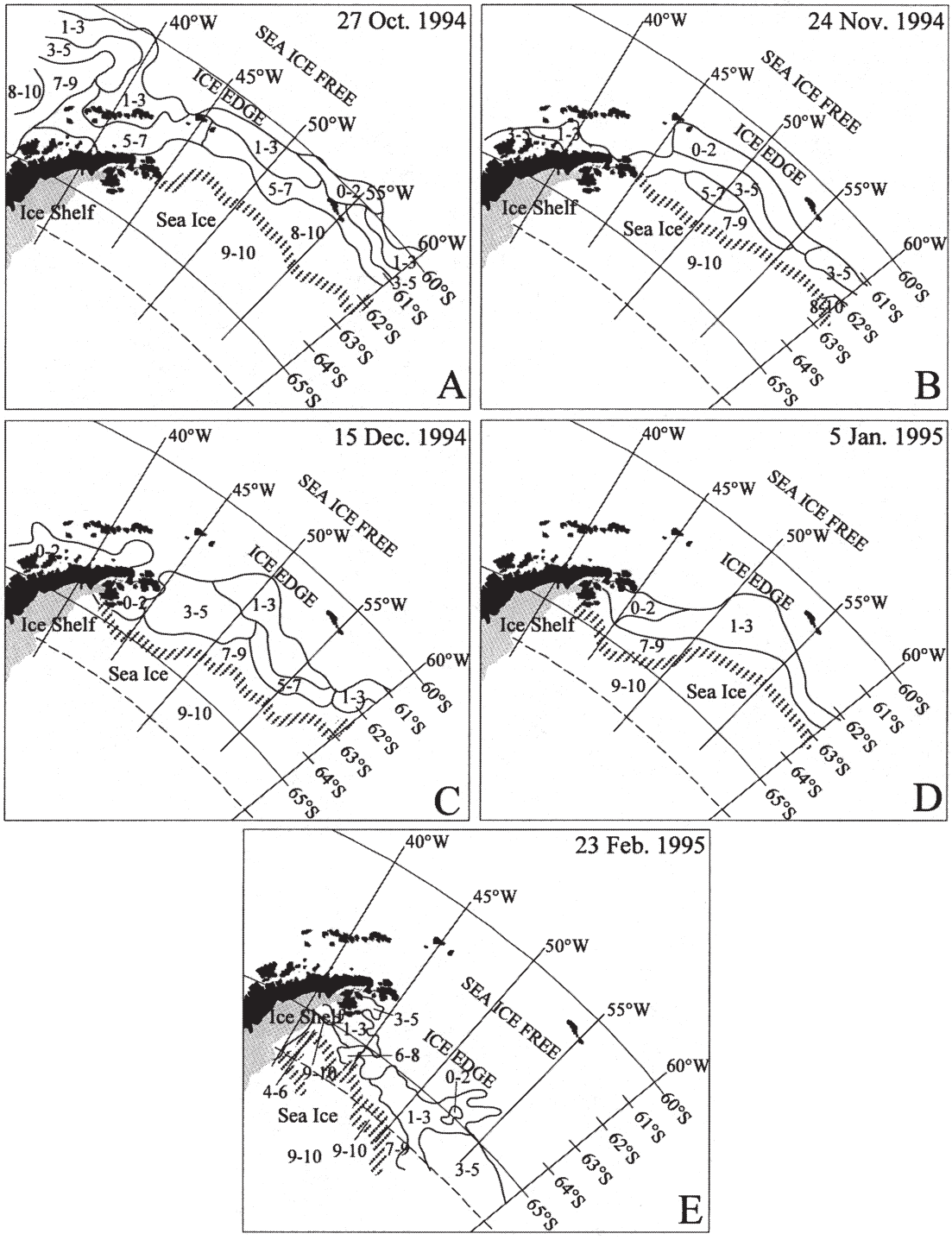

Fig. 2. (**A–E**) Areal and temporal extent of sea-ice cover near the sampling area from 27 October 1994 to 23 February 1995. The sea-ice cover images were produced by the US Navy–NOAA Joint Ice Center (JIC). The southern portion of the study region is typically covered with pack ice throughout the year, whereas the Bransfield Strait portion is ice free from early summer (approximately 24 November). The fraction of ice coverage is in tenths, i.e. 3–5 is equivalent to 30–50%.

subsequent phytoplankton growth. Satellite data indicate that the seasonal sea-ice cover started to melt back from the study area in late November 1994, and monthly time series show that melting progressed rapidly (Figure 2A–E). The northern part of the study area was <10% ice covered by 24 November 1994 over the study area in the Weddell Sea, and melting of the pack ice was pretty much complete by late February. Thus, the Bransfield Strait region, which was ice free longer than the Weddell Sea zone, had more time for upper waters to warm (Figure 2A–E).

Horizontal and vertical gradients

Hydrographic observations in the MIZ stations support previous models of meltwater-induced stratification of the water column (Smith and Nelson, 1986, 1990). We observed three characteristic surface water types (Figure 3A–I): (i) Bransfield Strait waters, with temperature generally >0°C and salinity 33.8–34.2 p.s.u.; (2) waters of Weddell Sea origin, with temperature <0°C and salinity (34.3–34.4 p.s.u.) higher than that of Bransfield Strait waters; (iii) Weddell Sea ice-edge waters, with lower temperature (<–0.2°C) and lower salinity (33.6–34.1 p.s.u.). Temperature varied from freezing (about –1.83°C) near the ice edge to warmer than –0.5°C toward the north of the study region (Figure 3A). The upper mixed layer comprises the Weddell surface water layer, which varies seasonally in its temperature and salinity characteristics. The underlying cold core is the Weddell winter water, a remnant from the preceding winter's cold convective layer

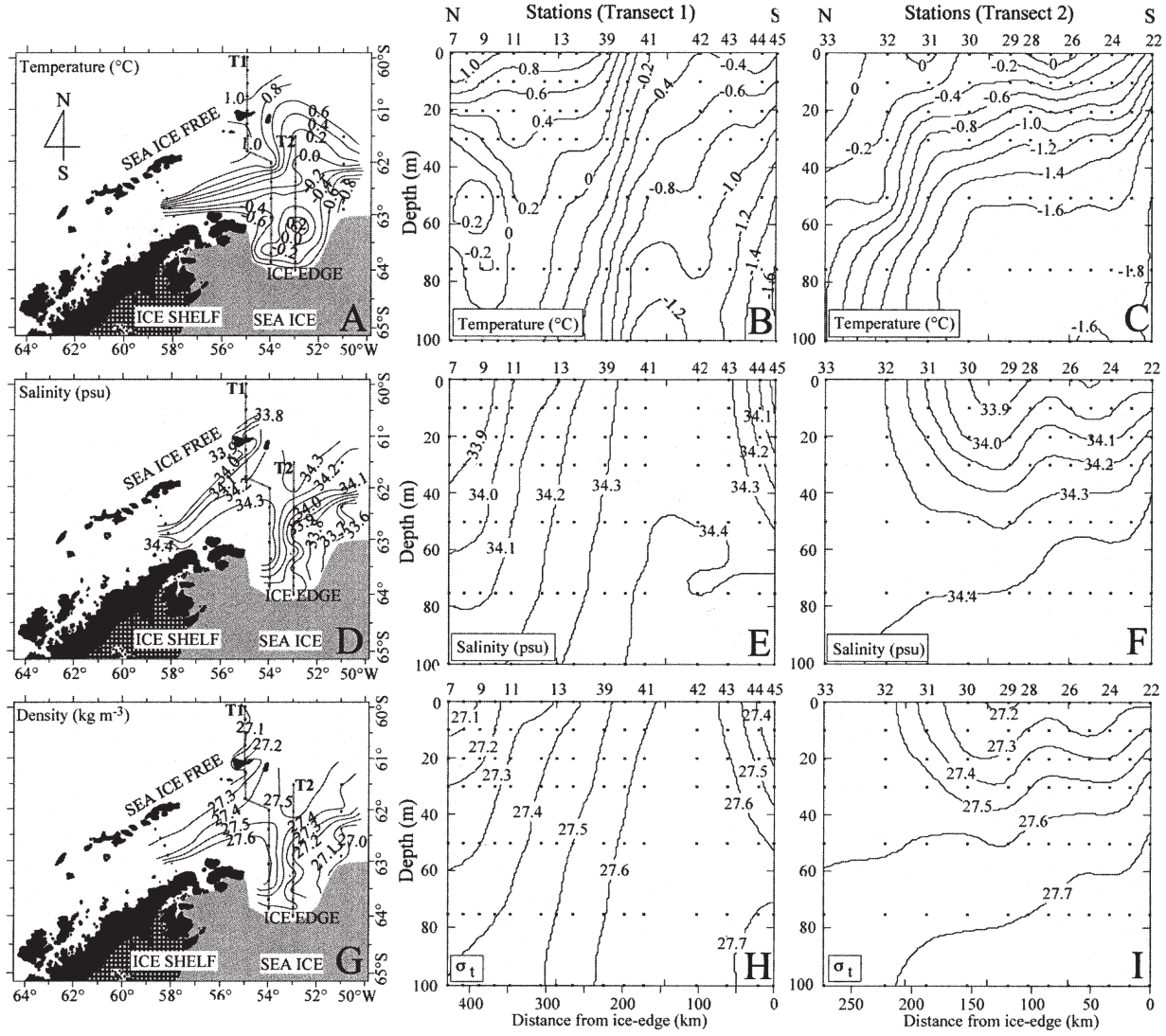

Fig. 3. Surface and vertical distributions of (**A–C**) temperature, (**D–F**) salinity and (**G–I**) σ_t contoured from data collected at 38 stations in the upper 100 m along Transect 1 and Transect 2.

(Figure 3B and C). Surface salinity was between 33.6 and 34.4 p.s.u., with the lower values (<33.8 p.s.u.) at the southern end (Weddell Sea MIZ) and northern end (lower salinity Bellingshausen water) (Figure 3D). A sharp halocline and pycnocline underlay the upper mixed layer, with salinity increasing to ~34.4 p.s.u. at ~50 m, which then increased gradually with depth (Figure 3E and F).

Inorganic nutrients and Chl *a* concentrations

Surface nitrate and silicate concentrations were low in the well-stratified waters adjacent to the ice edge and were high in Bransfield Strait (Figure 4A–F). The nutrient concentrations were inversely related to phytoplankton biomass (Figure 5A and B). A significant depletion of nitrate and silicate concentrations between Stations 22 and 31 along transect #2 coincided with the lens of low-salinity surface water. Nitrate and silicate along transect #1 were also significantly low near the ice edge (Figure 4B and E).

Typical Chl *a* concentrations in the stratified waters adjacent to the ice edge were >5 mg m^{-3} and reached as much as 13 mg m^{-3} in surface water samples in the MIZ (Figure 4G–I), illustrating the well-known relationship between surface water stratification and primary production (Sakshaug and Holm-Hansen, 1984; Garrison *et al.*, 1986; Smith and Nelson, 1986; Park *et al.*, 1999). The vertical distribution of phytoplankton was closely related to

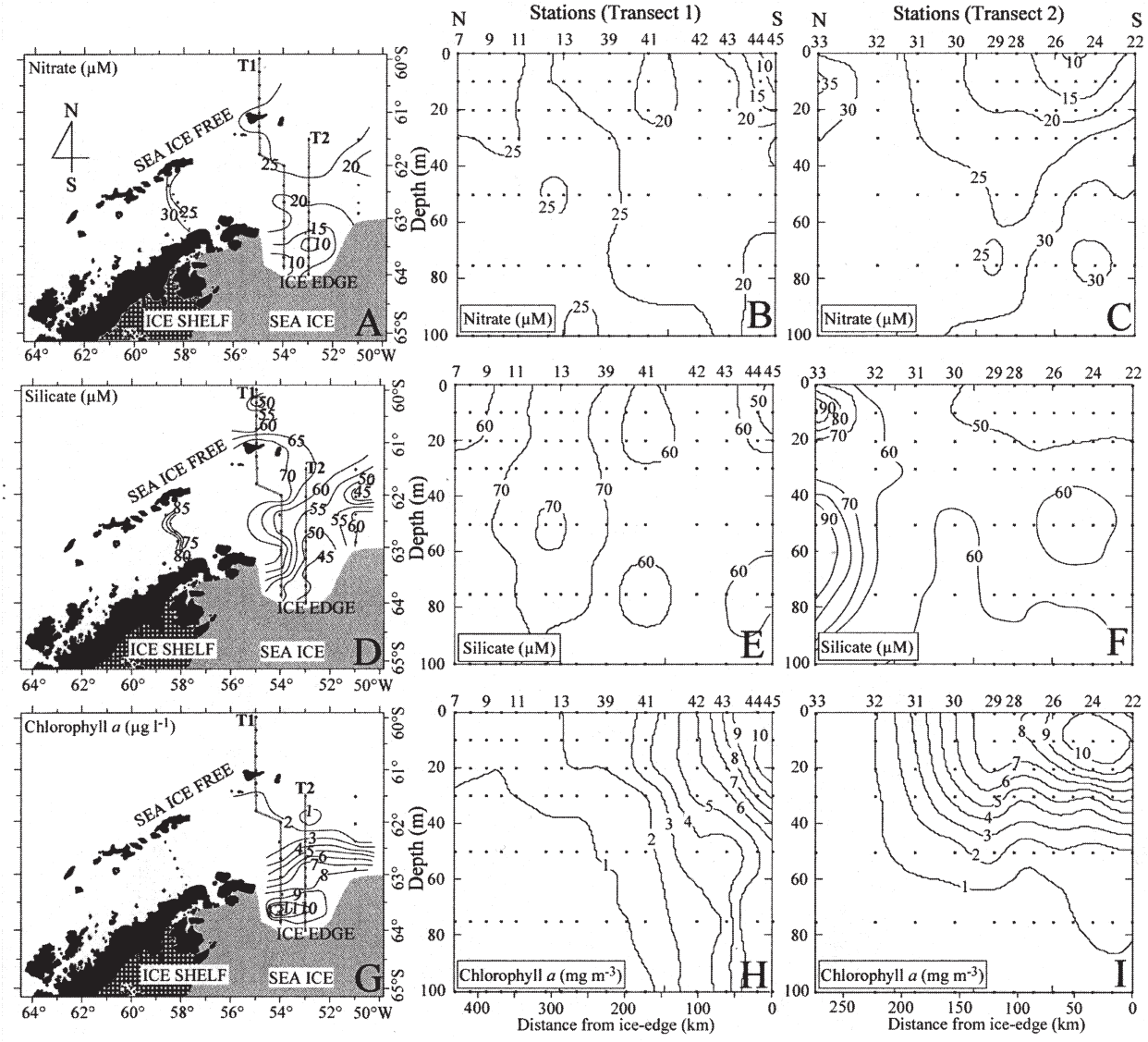

Fig. 4. Surface and vertical distributions of (**A–C**) nitrate, (**D–F**) silicate and (**G–I**) Chl *a* contoured from data collected at 38 stations in the upper 100 m along Transect 1 and Transect 2.

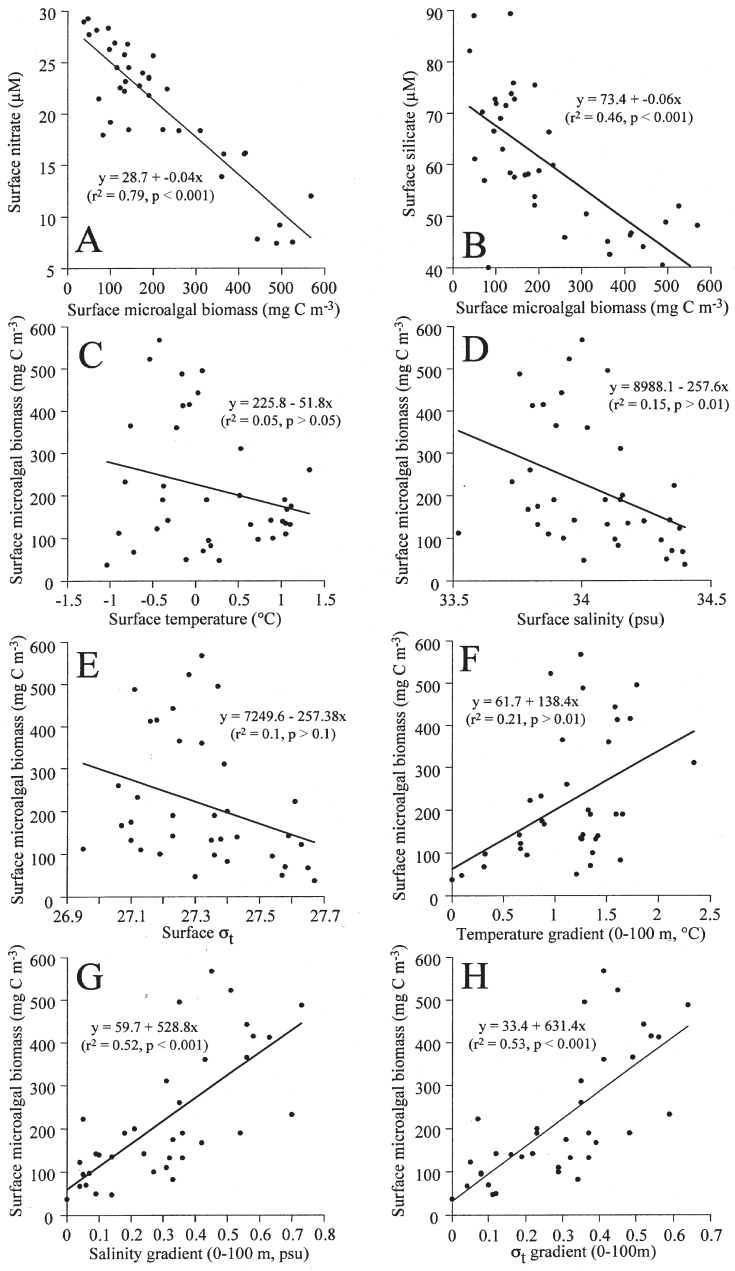

Fig. 5. Relationships (**A** and **B**) between surface microalgal biomass and nitrate and silicate, (**C–E**) between surface microalgal biomass and surface temperature, salinity and σ_t, and (**F–H**) between surface microalgal biomass and temperature, salinity and σ_t gradients.

hydrography, and was consistent with the nutrient distribution (Figures 3A–I and 4A–F).

Mesoscale distribution patterns of the phytoplankton standing crops and the dominant phytoplankton species

Phytoplankton comprised 65 species and groups of diatoms, and 10 species and groups of autotrophic flagellates (Table I). There was discernible spatial variation in the distribution of phytoplankton species and groups between open waters and the MIZ (Figures 6 and 7). Phytoplankton standing crops (abundance and C biomass) were highest in the MIZ of the Weddell Sea (Figure 6A–P). The distribution pattern of the abundance, C biomass and Chl *a* resembles the vertical and horizontal structure of the density field, and the peaks of the standing crops (>1.4 × 10^7 cells l^{-1}, >450 mg C m^{-3} and >10 mg Chl *a* m^{-3}, respectively) were usually

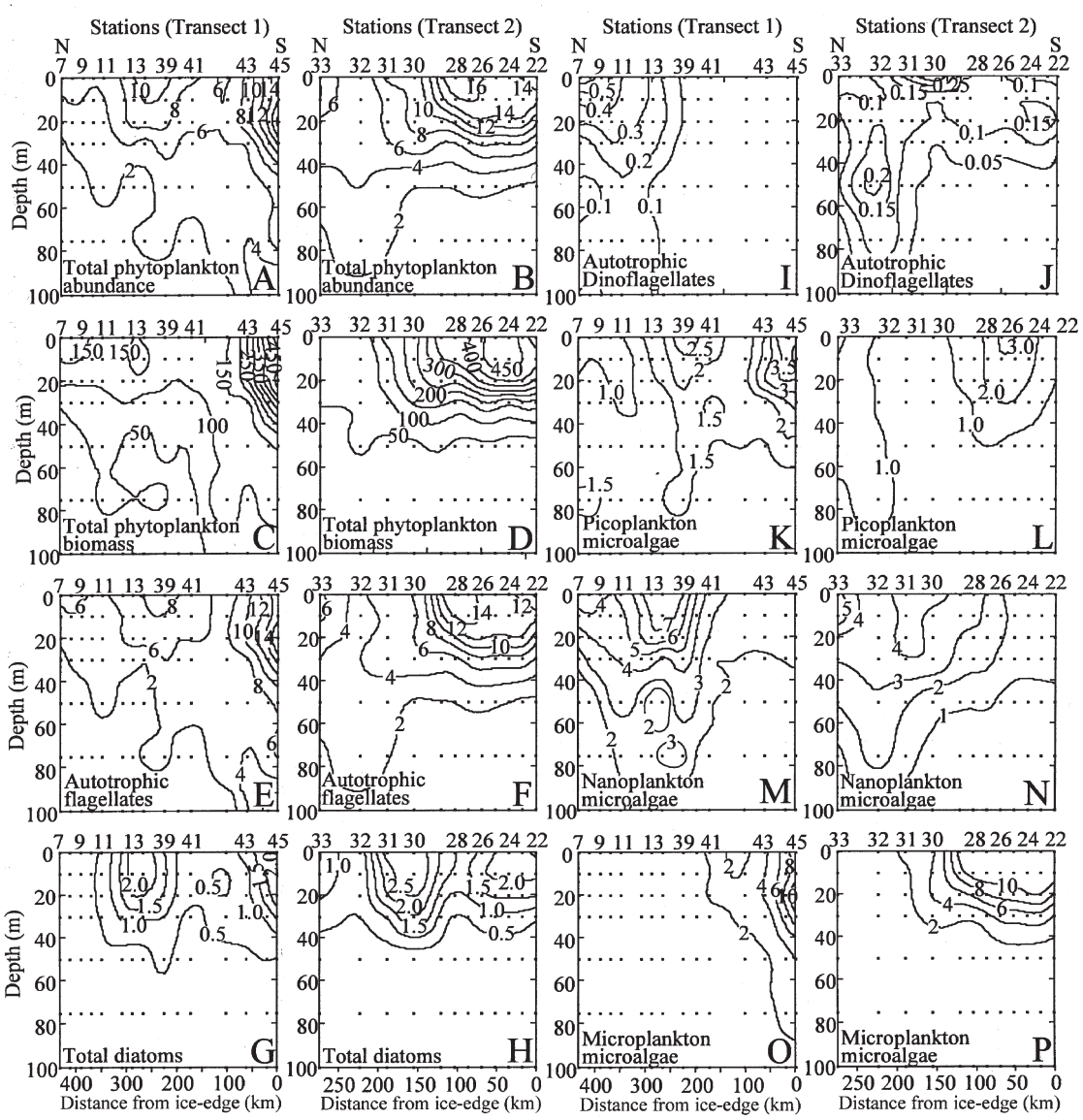

Fig. 6. Vertical sections of (**A** and **B**) total phytoplankton abundance (× 10^6 cells $^{-1}$), (**C** and **D**) total phytoplankton biomass (mg C m^{-3}), (**E** and **F**) autotrophic flagellates (× 10^6 cells l^{-1}), (**G** and **H**) total diatoms (× 10^6 cells l^{-1}), (**I** and **J**) autotrophic dinoflagellate (× 10^6 cells l^{-1}), (**K** and **L**) picoplankton microalgae (× 10^6 cells l^{-1}), (**M** and **N**) nanoplankton microalgae (× 10^6 cells l^{-1}) and (**O** and **P**) microplankton microalgae (× 10^6 cells l^{-1}) in the upper 100 m along Transect 1 and Transect 2.

found above the pycnocline in stratified waters in the MIZ.

Integrated phytoplankton cell abundance (PPA) and C biomass (PPC) (m^{-2} for the upper 100 m; Table II) ranged from 0.2 × 10^{12} to 1.01 × 10^{12} cells m^{-2} (average 0.5 × 10^{12} cells m^{-2}) and from 3.5 to 26 g C m^{-2} (average 9.6 g C m^{-2}), respectively. However, of the 70 phytoplankton species found, five accounted for 87% of the total PPA and 57% of the total PPC (Table II). Averaged over the entire study area, the motile stage of *Phaeocystis antarctica* was the most abundant in terms of cells (~31% of the total PPA), yet made up only 6% of the total PPC (Table II). Larger celled (>20 μm) diatom species such as *Proboscia truncata* constituted <0.01% of the total PPA, but accounted for 11% of the total PPC.

Total PPC ranged from 3.5 to 26 g C m^{-2} (mean 9.6 ± 5.3 g C m^{-2}). In transects #1 and #2, the total PPC was concentrated in the upper 40 m and near the ice edge (Figure 6C and D). The largest phytoplankton biomass was 536 mg C m^{-3} at the surface and 26 g C m^{-2} in the upper 100 m of Station 45 (Figure 6C). Generally, nanophytoplankton were most abundant, including

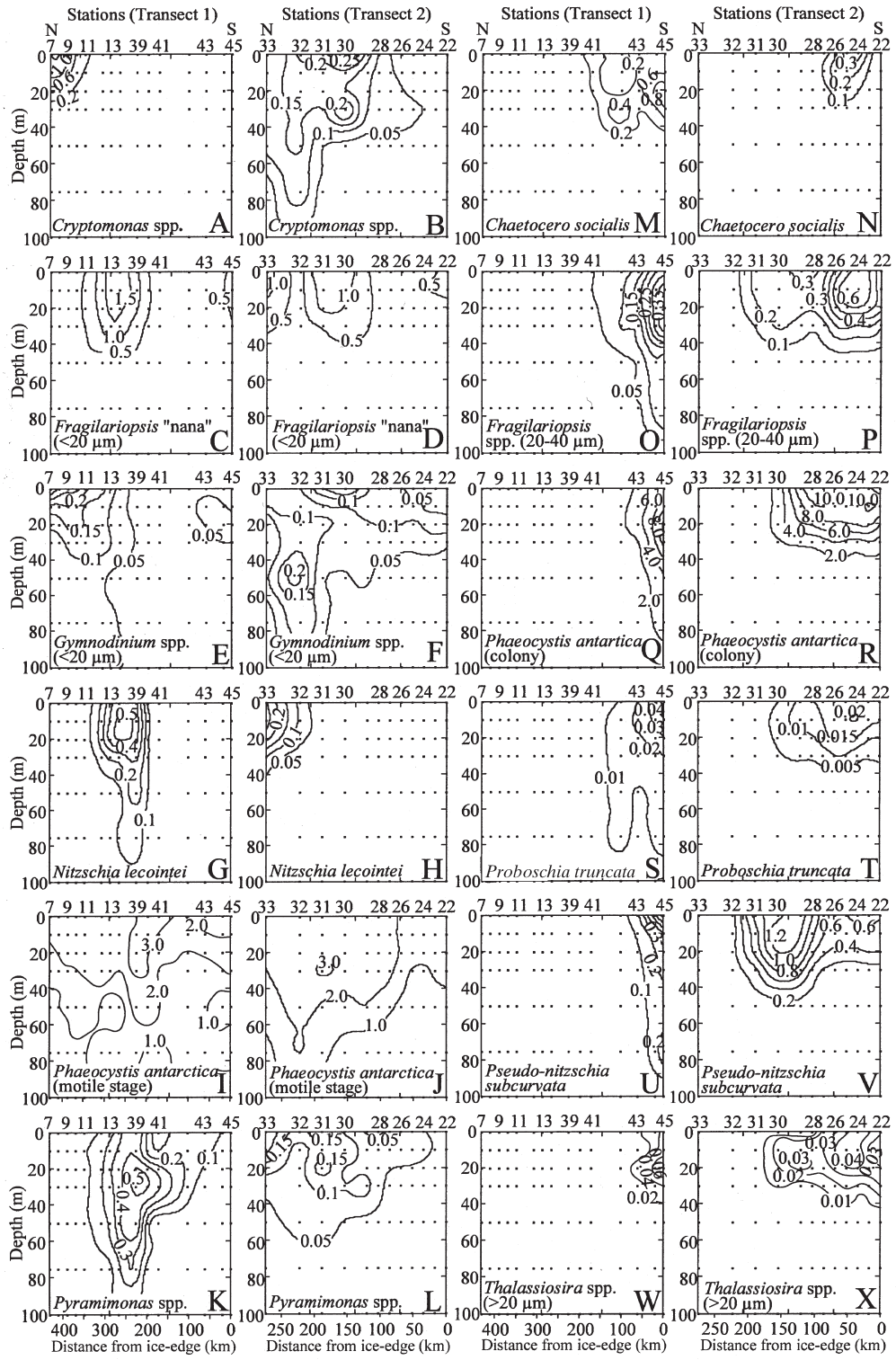

Fig. 7. (A–L) Vertical sections of dominant phytoplankton species abundance ($\times 10^6$ cells l^{-1}) in open waters near Bransfield Strait regions in the upper 100 m along Transect 1 and Transect 2. (**A** and **B**) *Cryptomonas* sp., (**C** and **D**) *Fragilariopsis* '*nana*' (mostly *F. pseudonana*), (**E** and **F**) *Gymnodinium* spp. (<20 μm), (**G** and **H**) *Nitzschia lecointei*, (**I** and **J**) *P. antarctica* in motile stage, (**K** and **L**) *Pyramimonas* spp. (M–X) Vertical sections of dominant phytoplankton species abundance ($\times 10^6$ cells l^{-1}) in the MIZ of the northwestern Weddell Sea in the upper 100 m along Transect 1 and Transect 2. (**M** and **N**) *Chaetoceros socialis*, (**O** and **P**) *Fragilariopsis* spp. (20–40 μm), (**Q** and **R**) *P. antarctica* in colonial stage, (**S** and **T**) *Proboscia truncata*, (**U** and **V**) *Pseudonitzschia subcurvata* and (**W** and **X**) *Thalassiosira* spp. (>20 μm).

Table II: Average abundance (PPA) and C biomass (PPC) of phytoplankton groups and size classes in 38 stations of the study area, January 1995

Station	Concentration ($\times 10^9$ cells m^{-2})						Carbon biomass (g C m^{-2})						Chl *a* (mg m^{-2})	
	auto	dtm	flg	pico	nano	micro	auto	dtm	flg	pico	nano	micro	Chl *a*	C/Chl *a*
1	325	14	311	82	236	7	5.0	0.4	4.6	0.1	3.4	1.5	81.0	61
2	487	19	468	144	327	16	9.2	0.4	8.8	0.1	5.4	3.6	85.8	107
3	514	22	492	128	371	15	10.2	0.4	9.9	0.1	6.9	3.3	101.7	101
4	222	6	216	96	117	9	4.0	0.2	3.8	0.1	2.0	2.0	60.7	66
5	378	15	363	200	168	9	4.4	1.5	2.9	0.1	2.2	2.1	86.7	51
6	202	13	189	77	86	39	6.0	4.4	1.6	0.1	0.8	5.2	119.6	50
7	291	18	274	88	194	9	5.6	0.4	5.3	0.1	3.5	2.1	94.4	60
8	269	14	255	67	193	9	5.4	0.3	5.1	0.1	3.2	2.1	83.1	64
9	454	20	434	168	273	13	7.0	0.4	6.6	0.1	4.1	2.9	78.6	90
10	327	13	314	70	245	12	6.2	0.3	5.9	0.1	3.6	2.5	74.9	83
11	514	44	471	104	389	21	9.1	1.0	8.1	0.1	4.8	4.3	96.1	94
12	473	41	432	89	369	15	7.7	1.0	6.7	0.1	4.5	3.1	83.5	92
13	503	123	380	112	358	33	7.8	3.4	4.4	0.1	4.3	3.4	129.7	60
14	246	63	183	32	195	19	4.2	1.5	2.7	0.0	2.6	1.6	90.7	46
33	379	50	329	124	242	12	4.2	2.2	2.0	0.1	2.5	1.6	71.7	58
34	876	402	474	76	797	3	11.3	7.2	4.1	0.1	10.6	0.6	143.9	78
39	856	130	727	253	555	49	9.9	4.8	5.2	0.2	6.1	3.7	168.2	59
22	470	63	407	71	107	292	13.6	8.2	5.4	0.1	1.0	12.5	384.4	35
23	640	75	565	81	87	472	16.4	7.9	8.5	0.1	0.9	15.4	523.0	31
24	456	66	391	82	72	302	13.5	8.4	5.1	0.1	0.7	12.8	347.7	39
25	513	68	445	102	82	329	16.5	10.8	5.7	0.1	0.8	15.7	406.6	41
26	631	79	552	188	71	372	16.7	10.4	6.3	0.1	0.8	15.7	433.0	38
27	635	29	606	117	200	318	10.6	3.7	7.0	0.1	1.6	9.0	235.3	45
28	490	41	449	79	126	286	9.2	3.3	5.9	0.1	1.3	7.8	245.2	37
29	703	112	591	60	311	333	15.2	8.5	6.7	0.0	2.4	12.7	443.3	34
30	418	117	301	70	197	151	9.0	5.8	3.2	0.1	2.4	6.5	257.8	35
31	405	81	325	64	272	70	6.0	3.1	2.8	0.0	2.8	3.2	161.1	37
37	554	84	469	59	225	269	9.6	3.1	6.5	0.0	2.9	6.6	309.3	31
32	383	23	360	115	258	10	4.8	1.6	3.2	0.1	3.2	1.5	77.1	62
42	561	47	514	156	183	222	15.4	10.6	4.8	0.1	1.2	14.1	438.9	35
43	538	37	501	158	200	180	10.3	6.0	4.3	0.1	1.1	9.1	398.3	26
44	729	90	639	228	108	393	22.1	15.4	6.7	0.2	0.7	21.3	986.8	22
45	1010	116	892	192	211	605	26.4	15.8	10.6	0.1	1.6	24.7	647.9	41
35	516	59	457	144	364	8	4.9	1.6	3.3	0.1	3.8	0.9	96.4	51
36	502	143	359	147	331	24	6.2	3.4	2.8	0.1	4.7	1.4	129.6	48
40	404	21	383	139	244	21	3.5	1.6	1.9	0.1	1.5	2.0	94.0	37
41	434	23	412	135	165	134	6.7	3.4	3.3	0.1	0.9	5.7	213.2	31
Average	495	64	431	116	241	137	9.6	4.4	5.2	0.1	2.9	6.6	229.2	53
		(13)	(87)	(23)	(49)	(28)		(46)	(54)	(1)	(30)	(69)		

auto, autotrophic phytoplankton; dtm, diatoms; flg, phytoflagellates; pico, picoplankton (<2 μm); nano, nanoplankton (2–20 μm); micro, microplankton (>20 μm).

P. antarctica, undetermined flagellates (4–5 μm), *Fragilariopsis* '*nana*' (<20 μm) and *Cryptomonas* sp., while the most important phytoplankton in terms of C biomass were micro-sized (>20 μm) species and groups such as *P. antarctica* in colonial stage, *P. truncata* Karsten, *Thalassiosira* spp., *Fragilariopsis* spp. and naked *Gymnodinium* spp. (Table II).

Diatoms

A total of 61 taxa of diatoms were identified (Table I), some as resting spores. Most taxa were most frequent in the Weddell Sea MIZ, whereas some occurred more commonly in open waters of the Bransfield Strait or in both environments (Figure 7). In the open waters of the Bransfield Strait region, *Nitzschia lecointei* Van Heurck, *Thalassiosira gracilis* (Karsten) Hustedt, *Fragilariopsis pseudonana* Hasle and *Rhizosolenia antennata* f. *semispina* Sundström were abundant (Figure 7A–L). However, *Thalassiosira* spp. [>20 μm: *T. gravida* Cleve, *T. ritscheri* (Hustedt) Hasle, *T. tumida* (Jan.) Fryxell and *T. antarctica* Comber], *Fragilariopsis* spp. [<20 μm: *F. cylindrus* (Grun.) Krieger; 20–40 μm: *F. curta* (V.H.) Hustedt.; and >40 μm: *F. obliquecostata* (V.H.) Hustedt, *F. ritscheri* (Hustedt) Hasle, *F. sublinearis* Hasle and *F. vanheurckii* (Per.) Hasle], *P. truncata*, *Chaetoceros* spp. (*C. neglectum* Karsten and *C. socialis* Lauder), *Pseudo-nitzschia* spp. [*P. heimii* Manguin, *P. lineola* Cleve/*P. turgiduloides* Hasle and *P. subcurvata* (Hasle) Fryxel] were more abundant in the MIZ (Figure 7M–X). Diatoms in the water column reached highest concentrations and biomass in the Weddell Sea MIZ, where pennate diatoms (principally *Pseudo-nitzschia* spp. and *Fragilariopsis* spp.) and centric species (primarily chain-forming colonies of *Thalassiosira* spp., *Chaetoceros* spp. and *Proboscia* spp.) were predominant. Diatoms made up 13% of autotrophic cells and 46% of autotrophic C.

Autotrophic nanoflagellates

Flagellates contributed 87% to autotroph cell number ($0.2–0.9 \times 10^{12}$ cells m^{-2}) and 54% to autotroph biomass (1.6–11 g C m^{-2}) in the upper 100 m (Table II). Overall, the colonial and flagellated stages of *P. antarctica* dominated the phytoplankton biomass (27% of the total biomass) at the chlorophyll maximum of the water column. The colonial stage of *P. antarctica* was more abundant in the Weddell Sea MIZ. Flagellates such as *Cryptomonas* spp., *Pyramimonas* spp. and *P. antarctica* in motile stage were more abundant in the open waters of the Bransfield Strait region (Figure 7A–L). Naked dinoflagellates (mainly *Gymnodinium* spp.), which was the second most important flagellate group (Figure 7E and F), contributed 16% to autotroph biomass. Autotrophic dinoflagellates comprised the size classes 5–20 and >20 μm. About 30% of the total autotrophic flagellate biomass, when viewed using EFM, comprised the autotrophic dinoflagellates. This group was severely underrepresented in the LM counts of previous studies [e.g. (Kang and Fryxell, 1993].

Phaeocystis antarctica

Phaeocystis antarctica (colonial and motile stages) was the most abundant species and important C contributor in the MIZ, accounting for 52% of total PPA and 27% of total PPC, respectively, which is comparable with the average biomass of *P. antarctica* from four seasonal cruises in the ice-edge zones reported earlier [(Kang, 1992); Table II]. The colonial stage of *P. antarctica* showed a peak in abundance in the MIZ (>1.0×10^7 cells l^{-1}) (Figure 7Q–R). The biomass of the colonial *P. antarctica* cells differed between the MIZ and the open waters; furthermore, *P. antarctica* showed a different distribution pattern depending on their life stages, as Kang and Kang (Kang and Kang, 1998) hypothesized. The colonial *P. antarctica* cells attained higher mean integrated biomass near the ice-edge stations, accounting for 3.6 g C m^{-2} (~30% of total PPC), whereas the motile *P. antarctica* dominated in the Bransfield Strait region, accounting for 0.6 g C m^{-2} (~9% of total PPC) (Figure 7I and J).

C/Chl *a* ratio

The distribution of PPC showed a similar pattern to that of Chl *a* concentration (Figures 4H and I and 6C and D). A good agreement was observed between PPC from microscopically enumerated counts and pigment concentration, showing a significant relationship ($r^2 = 0.8$, $P < 0.001$) (Figure 8). The average phytoplankton C:Chl *a* ratio in 37 stations was 53, ranging from 22 (Station 44) in the MIZ to 107 (Station 2) in the Bransfield Strait (Table II).

DISCUSSION

The hydrography indicates substantial differences between the open waters in the Bransfield Strait and the MIZ in the Weddell Sea. In the Bransfield area, mixed-layer depths varied from 60 to 100 m (Figure 3). In contrast, in the MIZ where the sea ice was retreating southwards, there was net melting, causing a uniform upper water column and a pycnocline depth between 20 and 40 m (Figures 2 and 3).

The phytoplankton species composition and abundance between the two regions also showed differences (Figures 6 and 7). Nanophytoplankton such as *Cryptomonas* sp., *N. lecointei*, *Thalassiosira* spp. (<20 μm; mostly *T. gracilis*), naked *Gymnodinium* spp., *Pyramimonas* spp., *Fragilariopsis* '*nana*' (<20 μm; mostly *F. pseudonana*), *Phaeocystis* in motile stage, and siliceous cysts were more abundant in the open waters of the Bransfield Strait region (Figure 7A–L). Schloss and Estrada (Schloss and Estrada, 1994), Kang and Lee (Kang and Lee, 1995) and Villafañe *et al.*

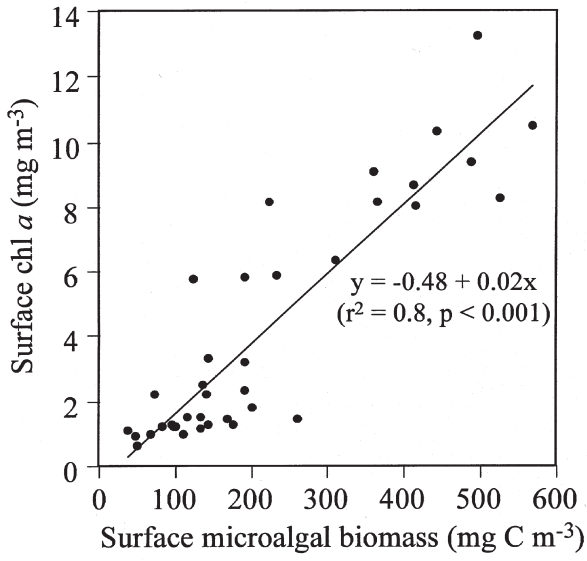

Fig. 8. Relationships between surface microalgal biomass and surface Chl *a*.

(Villafañe *et al.*, 1995) also observed high concentrations of nanophytoflagellates in the Bransfield Strait region. In contrast, microphytoplankton (mostly as colony- and/or chain-forming cells) such as *Chaetoceros neglectum*, *C. socialis*, *Fragilariopsis curta*, *F. cylindrus*, *F. sublinearis*, *F. obliquecostata*, *F. vanheurkii*, *P. antarctica* in colonial stage, *P. truncata*, *Pseudonitzschia* spp. (*P. heimii*, *P. lineola/turgiduloides* and *P. subcurvata*), *Thalassiosira* spp. (>20 μm: *T. gravida*, *T. tumida* and *T. ritscheri*) were more abundant in the MIZ (Figure 7M–X). These differences between the two regions could have resulted from different physicochemical conditions, such as depth of mixed layer, temperature, light limitation, micronutrient availability and biological removal processes that were degrading the phytoplankton increase with time and intensified grazing pressure and sinking.

The most important physical, chemical and biological factors controlling phytoplankton blooms in the Southern Ocean are the vertical stability of the water column (Mitchell and Holm-Hansen, 1991; Bianchi *et al.*, 1992; Veth *et al.*, 1992; Lancelot *et al.*, 1993), availability of trace metals [particularly iron (Martin *et al.*, 1990)] and grazing by macrozooplankton, krill (Smetacek *et al.*, 1990; Huntley *et al.*, 1991) and protozoa (Hewes *et al.*, 1990). Stability induced by meltwater seems to be the most important factor in our study area, as seen in the spatial coherence of the density field and elevated phytoplankton biomass (Figures 3 and 6). Moreover, we cannot completely exclude the possible roles of trace elements (particularly iron) and low grazing pressure (Smetacek and Passow, 1990; Sakshaug *et al.*, 1991) for the phytoplankton bloom adjacent to the northern end of the Antarctic Peninsula.

A cluster analysis was carried out in order to examine the relationships among the stations and their hydrographic regimes. Stations were treated as cases and the variables were the integrated PPC (mg C m^{-2}) of the most dominant species showing in Figure 7. The cluster analysis divided the study area into two major groups: stations (Cluster I) located in waters in the MIZ (Stations 40–45, 22–32 and 35–38) and stations (Cluster II) located in the eastern Bransfield Strait (Stations 1–5, 7–14, 34–35 and 39) (Figure 9).

The highest PPC was found in the stations of Cluster I (mean = 11.8 ± 6.1 g C m^{-2}) and the mean total PPC was ~1.7 times higher than that of the stations in Cluster II (Table III). Relatively high primary productivity and phytoplankton biomass have been observed in the MIZ of the northwestern Weddell Sea by Park *et al.* (Park *et al.*, 1999). They reported that the mean primary productivity in the MIZ (corresponding to Stations 22–31 in transect #2 and Station 44) was 3.7 times greater than that in open waters of the Bransfield region (Stations 32 and 33), suggesting that the MIZ was a major productive site, as reported by several previous studies in the Ross and Weddell Seas (Wilson *et al.*, 1986; Smith and Nelson, 1990). The mean productivity (2.1 g C m^{-2} day^{-1}) for the MIZ bloom during this study is an order of magnitude higher than means reported for the ice-edge bloom in the Ross and Weddell Seas during the growth season (Park *et al.*, 1999). The MIZ may make a significant contribution to the Southern Ocean productivity during summer.

Correlation statistics for the relationship between the physical factors and the phytoplankton populations indicate that in the MIZ stations microphytoplankton were significantly correlated with salinity and σ_t gradients ($P < 0.05$), but nanophytoplankton were not (Table IV). Surface waters in the Cluster I region are characterized by a strong vertical stratification caused by melting of sea ice. Cluster II stations, in contrast, are characterized by monotonous temperature decrease and salinity increase from the surface to the bottom (Figure 10), and the temperature in the upper 100 m was relatively high (–1.05 to 1.32°C), as was salinity (33.79–34.43 p.s.u.). Thus, the gradients in temperature, salinity and density were smaller than in the Cluster I stations, resulting in a vertically less stratified upper water column compared to the MIZ waters.

The two north–south transects (T1 and T2) are characterized by a frontal system (the Weddell–Bransfield Confluence) separating the eastward-flowing waters of the Bransfield Current from the northern branch of the northwestern Weddell Sea. The zone of well-stratified surface water was restricted to a belt ~100–180 km wide along the ice margin. Surface salinity distribution shows that the well-stratified surface waters were apparently

Table III: Average abundance (PPA) and C biomass (PPC) of phytoplankton groups and size classes between the MIZ stations in the Weddell Sea (Cluster I) and open-water stations in the Bransfield Strait region (Cluster II) of the study area, January 1995

Station	Concentration ($\times 10^9$ cells m^{-2})						Carbon biomass (g C m^{-2})						Chl *a* (mg m^{-2})	
	auto	dtm	flg	pico	nano	micro	auto	dtm	flg	pico	nano	micro	Chl *a*	C/Chl *a*
MIZ stations (Cluster I)														
22	470	63	407	71	107	292	13.6	8.2	5.4	0.1	1.0	12.5	384.4	35
23	640	75	565	81	87	472	16.4	7.9	8.5	0.1	0.9	15.4	523.0	31
24	456	66	391	82	72	302	13.5	8.4	5.1	0.1	0.7	12.8	347.7	39
25	513	68	445	102	82	329	16.5	10.8	5.7	0.1	0.8	15.7	406.6	41
26	631	79	552	188	71	372	16.7	10.4	6.3	0.1	0.8	15.7	433.0	38
27	635	29	606	117	200	318	10.6	3.7	7.0	0.1	1.6	9.0	235.3	45
28	490	41	449	79	126	286	9.2	3.3	5.9	0.1	1.3	7.8	245.2	37
29	703	112	591	60	311	333	15.2	8.5	6.7	0.0	2.4	12.7	443.3	34
30	418	117	301	70	197	151	9.0	5.8	3.2	0.1	2.4	6.5	257.8	35
31	405	81	325	64	272	70	6.0	3.1	2.8	0.0	2.8	3.2	161.1	37
37	554	84	469	59	225	269	9.6	3.1	6.5	0.0	2.9	6.6	309.3	31
32	383	23	360	115	258	10	4.8	1.6	3.2	0.1	3.2	1.5	77.1	62
42	561	47	514	156	183	222	15.4	10.6	4.8	0.1	1.2	14.1	438.9	35
43	538	37	501	158	200	180	10.3	6.0	4.3	0.1	1.1	9.1	398.3	26
44	729	90	639	228	108	393	22.1	15.4	6.7	0.2	0.7	21.3	986.8	22
45	1010	116	892	192	211	605	26.4	15.8	10.6	0.1	1.6	24.7	647.9	41
35	516	59	457	144	364	8	4.9	1.6	3.3	0.1	3.8	0.9	96.4	51
36	502	143	359	147	331	24	6.2	3.4	2.8	0.1	4.7	1.4	129.6	48
40	404	21	383	139	244	21	3.5	1.6	1.9	0.1	1.5	2.0	94.0	37
41	434	23	412	135	165	134	6.7	3.4	3.3	0.1	0.9	5.7	213.2	31
Average	550	69	481	119	191	240	11.8	6.6	5.2	0.1	1.8	9.9	341	38
		(12)	(88)	(21)	(35)	(44)		(56)	(44)	(1)	(15)	(84)		
Open-water stations (Cluster II)														
1	325	14	311	82	236	7	5.0	0.4	4.6	0.1	3.4	1.5	81.0	61
2	487	129	468	144	327	16	9.2	0.4	8.8	0.1	5.4	3.6	85.8	107
3	514	22	492	128	371	15	10.2	0.4	9.9	0.1	6.9	3.3	101.7	101
4	222	6	216	96	117	9	4.0	0.2	3.8	0.1	2.0	2.0	60.7	66
5	378	15	363	200	168	9	4.4	1.5	2.9	0.1	2.2	2.1	86.7	51
6	202	13	189	77	86	39	6.0	4.4	1.6	0.1	0.8	5.2	119.6	50
7	291	18	274	88	194	9	5.6	0.4	5.3	0.1	3.5	2.1	94.4	60
8	269	14	255	67	193	9	5.4	0.3	5.1	0.1	3.2	2.1	83.1	64
9	454	20	434	168	273	13	7.0	0.4	6.6	0.1	4.1	2.9	78.6	90
10	327	13	314	70	245	12	6.2	0.3	5.9	0.1	3.6	2.5	74.9	83
11	514	44	471	104	389	21	9.1	1.0	8.1	0.1	4.8	4.3	96.1	94
12	473	41	432	89	369	15	7.7	1.0	6.7	0.1	4.5	3.1	83.5	92
13	503	123	380	112	358	33	7.8	3.4	4.4	0.1	4.3	3.4	129.7	60
14	246	63	183	32	195	19	4.2	1.5	2.7	0.0	2.6	1.6	90.7	46
33	379	50	329	124	242	12	4.2	2.2	2.0	0.1	2.5	1.6	71.7	58
34	876	402	474	76	797	3	11.3	7.2	4.1	0.1	10.6	0.6	143.9	78
39	856	130	727	253	555	49	9.9	4.8	5.2	0.2	6.1	3.7	168.2	59
Average	430	59	371	112	301	17	6.9	1.7	5.2	0.1	4.1	2.7	97	72
		(14)	(86)	(26)	(70)	(4)		(25)	(75)	(1)	(60)	(39)		

auto, autotrophic phytoplankton; dtm, diatoms; flg, phytoflagellates; pico, picoplankton (<2 μm); nano, nanoplankton (2–20 μm); micro, microplankton (>20 μm). Numbers in parentheses show the percentage of total PPA and total PPA.

Table IV: Pearson correlation matrix of biological or environmental parameters from the top 100 m between the MIZ stations in the Weddell Sea (Cluster I) and open-water stations in the Bransfield Strait region (Cluster II)

	Temp	TempGr	Sal	SalGr	Den	DenGr	NO_3	$SiOH_4$	Bac	Chla	PicoC	NanoC	MicroC	FlC	DtmC	PPC
MIZ stations (Cluster I)																
Temp	1.00-	–	–	–	–	–	–	–	–	–	–	–	–	–	–	–
TempGr	0.83	1.00	–	–	–	–	–	–	–	–	–	–	–	–	–	–
Sal			1.00	–	–	–	–	–	–	–	–	–	–	–	–	–
SalGr			–1.00	1.00	–	–	–	–	–	–	–	–	–	–	–	–
Den			1.00	–1.00	1.00	–	–	–	–	–	–	–	–	–	–	–
DenGr			–0.99	0.99	–1.00	1.00	–	–	–	–	–	–	–	–	–	–
NO_3				–0.50		–0.51	1.00	–	–	–	–	–	–	–	–	–
$SiOH_4$		–0.57		–0.68	0.44	–0.72	0.65	1.00	–	–	–	–	–	–	–	–
Bac							–0.59		1.00	–	–	–	–	–	–	–
Chla				0.50		0.49	–0.81			1.00	–	–	–	–	–	–
PicoC							–0.78		0.58	0.68	1.00	–	–	–	–	–
NanoC			–0.46		–0.45		0.59		–0.48	–0.55	–0.69	1.00	–	–	–	–
MicroC				0.58		0.59	–0.89	–0.56	0.50	0.91	0.65	–0.58	1.00	–	–	–
FlC			–0.45	0.66	–0.48	0.69	–0.46	–0.53		0.54			0.69	1.00	–	–
DtmC				0.49		0.48	–0.89	–0.47	0.49	0.89	0.76	–0.52	0.92		1.00	–
PPC				0.65		0.66	–0.87	–0.58	0.46	0.90	0.59	–0.47	0.99	0.72	0.92	1.00
Open-water stations (Cluster II)																
Temp	1.00	–	–	–	–	–	–	–	–	–	–	–	–	–	–	–
TempGr	0.55	1.00	–	–	–	–	–	–	–	–	–	–	–	–	–	–
Sal	–0.70		1.00	–	–	–	–	–	–	–	–	–	–	–	–	–
SalGr	0.64		–0.89	1.00	–	–	–	–	–	–	–	–	–	–	–	–
Den	–0.78		0.99	–0.89	1.00	–	–	–	–	–	–	–	–	–	–	–
DenGr	0.73	0.54	–0.83	0.97	–0.85	1.00	–	–	–	–	–	–	–	–	–	–
NO_3	–0.66	–0.57	0.60	–0.63	0.65	–0.71	1.00	–	–	–	–	–	–	–	–	–
$SiOH_4$							0.54	1.00	–	–	–	–	–	–	–	–
Bac			–0.53		–0.50				1.00	–	–	–	–	–	–	–
Chla		0.72								1.00	–	–	–	–	–	–
PicoC			0.62		0.59						1.00	–	–	–	–	–
NanoC		0.63				0.50	–0.49	–0.56				1.00	–	–	–	–
MicroC	0.57				–0.51		–0.56	–0.46					1.00	–	–	–
FlC	0.62		–0.67	0.75	–0.69	0.76	–0.73	–0.68				0.71	0.72	1.00	–	–
DtmC			0.58		0.51				–0.69	0.76					1.00	–
PPC	0.62	0.60		0.53		0.62	–0.64	–0.65				0.88	0.68	0.89		1.00

Temp, temperature; TempGr, temperature gradient between 0 and 100 m; Sal, salinity; SalGr, salinity gradient; Den, σ_t; DenGr, σ_t gradient; NO_3, nitrate; $SiOH_4$, silicate; Bac, bacterioplankton carbon biomass; Chla, Chl *a*; PicoC, picoplankton carbon biomass; NanoC, nanoplankton carbon biomass; MicroC, microplankton carbon; FlC, phytoflagellate carbon biomass; DtmC, diatom carbon biomass; PPC, total phytoplankton carbon biomass. *R* values shown are significant ($P \leq 0.05$); values where $P > 0.05$ are not presented.

flowing out of waters from the northwestern Weddell Sea surface water. During January, low-salinity waters (<34.0 p.s.u.) in the Weddell Sea met high-salinity waters in a front along the northeastern extension of the Antarctic Peninsula. Sea surface temperature varied only from –1.04 to +1.32°C, the density (σ_t) distribution along each transect was largely a function of the salinity. Low-density (<27.2) surface waters were well developed offshore (eastern transects) from the Antarctic Peninsula within the MIZ. Near the MIZ, the water column was more stratified with distinct pycnoclines between 20 and 40 m depth (σ_t gradients >0.6 with mean of 0.37 ± 0.19) between

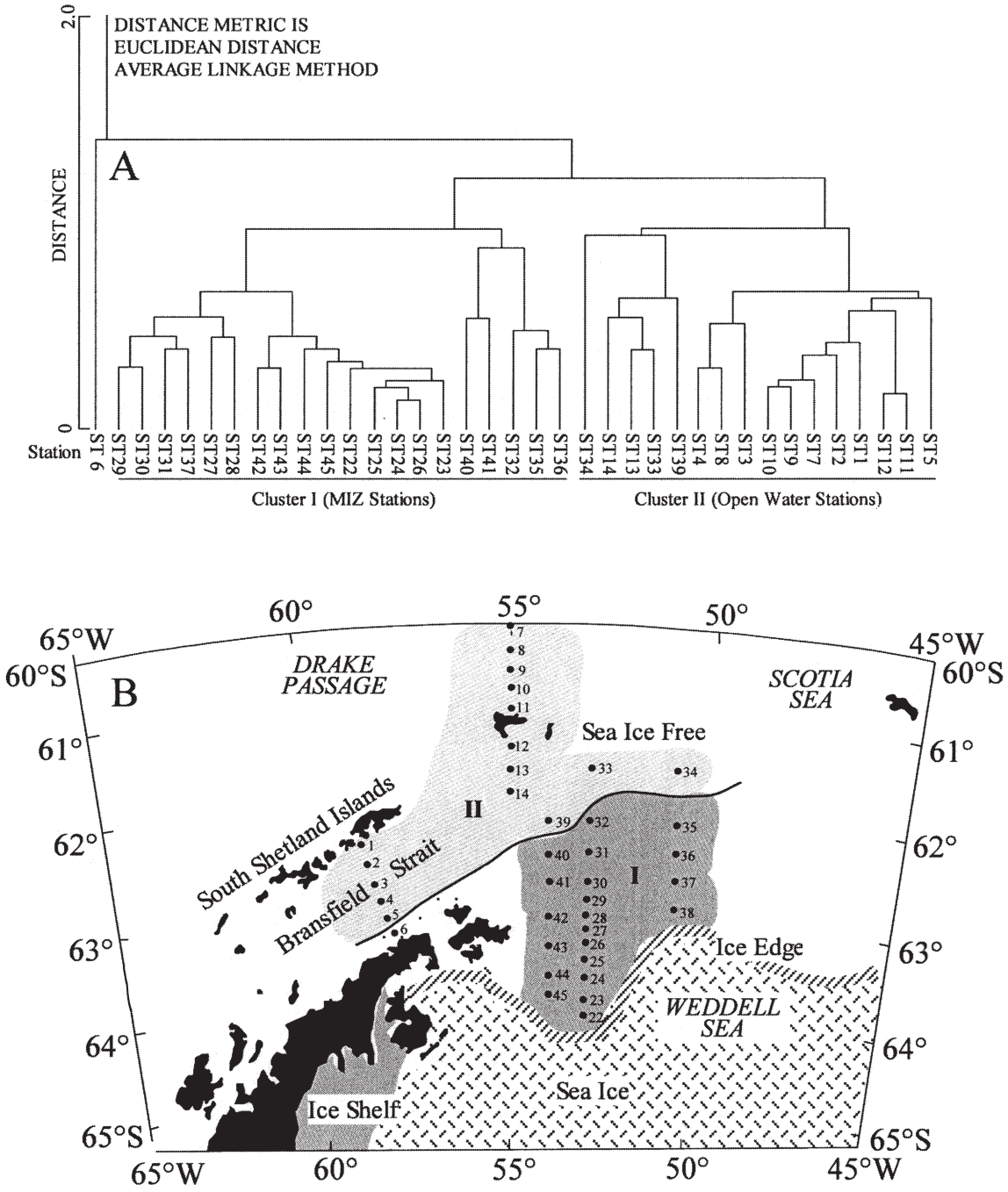

Fig. 9. (**A**) Dendrogram from the average-linkage analysis on stations. Variables for the analysis were the integrated C biomass of phytoplankton species and groups in Figure 7. See Method for details of the analysis. (**B**) Location of the clusters in the study area.

0 and 100 m. At the open-water stations north of the Weddell–Bransfield front, the difference was only 0.23 ± 0.11 between 0 and 100 m depth. Phytoplankton concentrations above the pycnoclines (shallower mixed-layer depths) were high in the MIZ but low in the open-water stations in the Bransfield Strait. The σ_t gradient was more significantly correlated with phytoplankton biomass (r^2 = 0.53, $P < 0.001$) than other physical factors (Figure 5C–H), suggesting that large phytoplankton biomasses were associated with the strong vertical stratification.

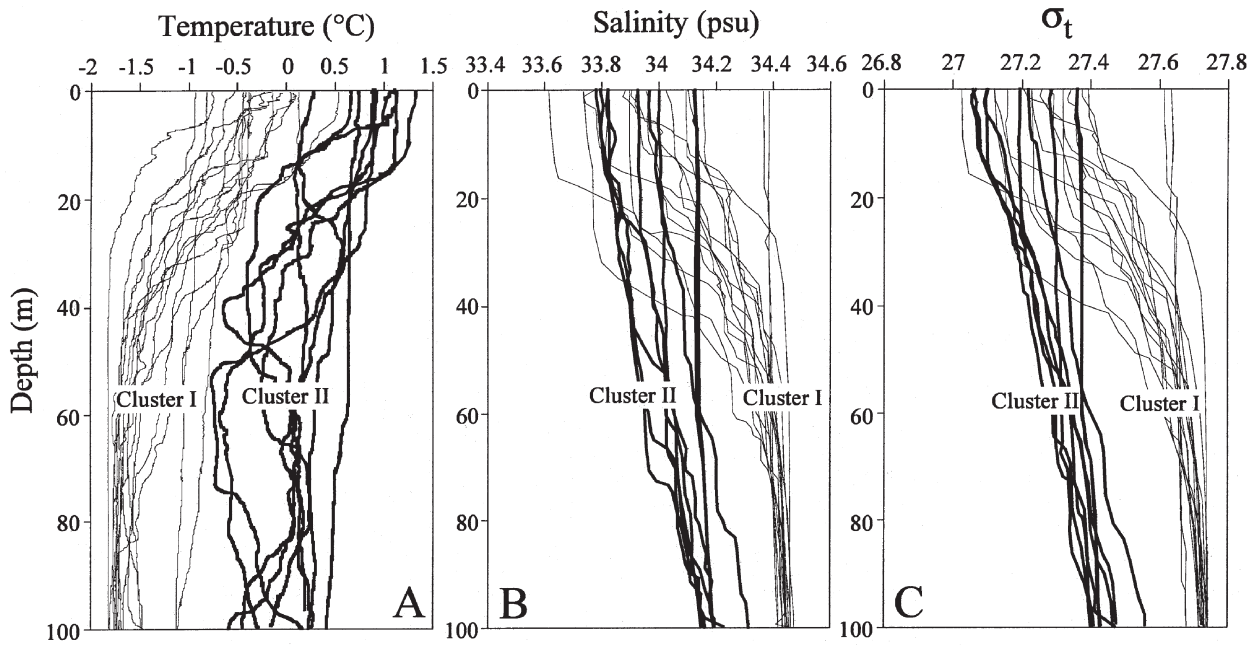

Fig. 10. Vertical profiles of (**A**) temperature, (**B**) salinity and (**C**) σ_t on the two clusters of Figure 9.

CONCLUSIONS

Phytoplankton communities in the study area were diverse in species, and comprised a wide range of cell sizes. Phytoplankton assemblages showed a marked contrast between the northwestern Weddell Sea MIZ and open water of the eastern Bransfield Strait. Waters in the Bransfield Strait were characterized by a dominance of nanoflagellates such as *Cryptomonas* sp., *Phaeocystis antarctica* in motile stage, *Pyramimonas* spp. and naked *Gymnodinium* spp. (<20 μm), accounting for 80% of the total phytoplankton C. In the Weddell Sea MIZ, however, colonial stage of *P. antarctica* and micro-sized chain-forming diatoms such as *Chaetoceros* spp., *Thalassiosira* spp., *Pseudo-nitzschia* spp. and *Fragilariopsis* spp. accounted for 70% of the total phytoplankton C. These data should be useful as a baseline for the northwestern Weddell Sea region.

Cluster analysis using the integrated PPC (mg C m^{-2}) of the most dominant phytoplankton species and groups of related species enumerated from discrete water samples from the ice-edge zone not only separated them based on depth (above the pycnocline versus below the pycnocline in the most productive area), but also separated them based on location in the ice-edge zone (ice-related waters versus open waters in the Bransfield Strait) in this dynamic season. Regional differences in the structure of phytoplankton assemblages, whether a flagellate-dominated (Cluster II) crop or a diatom-dominated crop (Cluster I), appear to reflect the differences in water mass properties, such as time scale of mixing stratification and duration of a shallow mixed layer. Antarctic phytoplankton species dominant under certain environmental conditions could be extended to a 'marker' that distinguishes water bodies among varying hydrographic regimes.

ACKNOWLEDGEMENTS

We thank the captain and crew members of RV 'Yuzhmorgeologiya' for help during the cruise. We also thank Mr I. H. Lee, D. W. Park and M. Y. Lee for assistance in fieldwork. We are grateful to the members of the 8th Korean Antarctic Research Program for their technical and emotional support. Special thanks go to Ms Eun Jung Kim and Ms Adele Kim who helped to improve the manuscript. This work was supported by the KORDI project PP9900104 and PN99385.

REFERENCES

Arrigo, K. R., Worthen, D., Schnell, A. and Lizotte, M. P. (1998) Primary production in southern ocean waters. *J. Geophys. Res.*, **103**, 15587–15600.

Bianchi, F. *et al.* (1992) Phytoplankton distribution in relation to sea ice, hydrography and nutrients in the northwestern Weddell Sea in early spring 1988 during EPOS. *Polar Biol.*, **12**, 225–235.

Bidigare, R. R., Iriarte, J. L., Kang, S.-H., Karentz, D., Ondrusek, M. E. and Fryxell, G. A. (1996) Phytoplankton: Quantitative and qualitative assessments. In Ross, R. M., Hofmann, E. E. and Quetin, L. B. (eds) *Foundation for Ecological Research of the Antartic Peninsula. Antarct. Res. Ser.*, **70**, 173–198.

Capella, J. E., Quetin, L. B., Hofmann, E. E. and Ross, R. M. (1992) Models of the early life history of *Euphausia superba*—Part II. Lagrangian calculations. *Deep-Sea Res.*, **39**, 1201–1220.

Cota, G. F., Smith, W. O., Jr, Nelson, D. M., Muench, R. D. and Gordon, L. I. (1992) Nutrient and biogenic particulate distributions, primary productivity and nitrogen uptake in the Weddell–Scotia Sea marginal ice zone during winter. *J. Mar. Res.*, **50**, 155–181.

Crumpton, W. G. (1987) A simple and reliable method for making permanent mounts of phytoplankton for light and fluorescence microscopy. *Limnol. Oceanogr.*, **32**, 1154–1159.

Fryxell, G. A. and Kendrick, G. A. (1988) Austral spring microalgae across the Weddell Sea ice edge: spatial relationships found along a northward transect during AMERIEZ 83. *Deep-Sea Res.*, **35**, 1–20.

Garrison, D. L., Sullivan, C. W. and Ackley, S. F. (1986) Sea ice microbial communities in Antarctica. *Biol. Sci.*, **36**, 243–250.

Garrison, D. L., Buck, K. R. and Fryxell, G. A. (1987) Algal assemblages in Antarctic pack ice and in ice-edge plankton. *J. Phycol.*, **23**, 564–572.

Garrison, D. L., Buck, K. R. and Gowing, M. M. (1993) Winter plankton assemblage in the ice edge zone of the Weddell and Scotia Seas: composition, biomass and spatial distributions. *Deep-Sea Res.*, **40**, 311–338.

Gould, R. W., Jr (1987) The horizontal and vertical distribution of phytoplankton in warm core ring 82B. A five-month time series. PhD Dissertation, Texas A&M University, College Station, TX, 180 pp.

Grasshoff, K., Ehrhardt, M. and Kremling, K. (1983) *Methods of Seawater Analysis*. Verlag Chemie, Weinheim.

Hewes, C. D., Sakshaug, E., Reid, F. M. H. and Holm-Hansen, O. (1990) Microbial autotrophic and heterotrophic eucaryotes in Antarctic waters: relationships between biomass and chlorophyll, adenosine triphosphate and particulate organic carbon. *Mar. Ecol. Prog. Ser.*, **63**, 27–35.

Hewitt, R. P. (1997) Areal and seasonal extent of sea-ice cover off the northwestern side of the Antarctic Peninsula: 1979 to 1996. *CCAMLR Sci.*, **4**, 65–73.

Hofmann, E. E., Lascara, C. M. and Klinck, J. M. (1992) Palmer LTER: Upper-ocean circulation in the LTER region from historical sources. *Antarct. J. US*, **27**, 239–241.

Hofmann, E. E., Klinck, J. M., Lascara, C. M. and Smith, D. A. (1996) Water mass distribution and circulation west of the Antarctic Peninsula and including Bransfield Strait. In Ross, R. M., Hofmann, E. E. and Quetin, L. B. (eds), *Foundations for Ecological Research West of the Antarctic Peninsula. Antarct. Res. Ser.*, **70**, 81–104.

Holm-Hansen, O. and Mitchell, B. G. (1991) Spatial and temporal distribution of phytoplankton and primary production in the western Bransfield Strait region. *Deep-Sea Res.*, **38**, 961–980.

Huntley, M., Karl, D. M., Niiler, P. and Holm-Hansen, O. (1991) Research on Antarctic Coastal Ecosystem Rates (RACER): an interdisciplinary field experiment. *Deep-Sea Res.*, **38**, 911–941.

Kang, S.-H. (1992) Phytoplankton in water column assemblages of Antarctic marginal ice edge zones. PhD Dissertation, Texas A&M University, College Station, TX, 272 pp.

Kang, S.-H. and Fryxell, G. A. (1991) Most abundant diatom species in water column assemblages from five ODP Leg 119 drill sites in Prydz Bay, Antarctica: Distributional patterns. In Barron, J. and Larsen, B. (eds), *Proceeding of the Ocean Drilling Program, Scientific Results, 119*. Ocean Drilling Program, College Station, TX, pp. 645–666.

Kang, S.-H. and Fryxell, G. A. (1992) *Fragilariopsis cylindrus* (Grunow) Krieger: The most abundant diatom in water column assemblages of Antarctic marginal ice edge zones. *Polar Biol.*, **12**, 609–627.

Kang, S.-H. and Fryxell, G. A. (1993) Phytoplankton in the Weddell Sea, Antarctica: Composition, abundance and the distribution in water column assemblages of the marginal ice-edge zone during austral autumn. *Mar. Biol.*, **116**, 335–352.

Kang, S.-H. and Kang, J. S. (1998) *Phaeocystis antarctica* Karsten as an indicator species of environmental changes in the Antarctic. *Korean J. Polar Res.*, **9**, 17–35.

Kang, S.-H. and Lee, S. H. (1995) Antarctic phytoplankton assemblage in the western Bransfield Strait region, February, 1993: composition, biomass, and mesoscale distributions. *Mar. Ecol. Prog. Ser.*, **129**, 253–267.

Kang, S.-H., Fryxell, G. A. and Roelke, D. L. (1993a) *Fragilariopsis cylindrus* compared with other species of the diatom family Bacillariaceae in Antarctic marginal ice edge zones. *Nova Hedwigia*, **106**, 335–352.

Kang, S.-H., Suk, M. S., Chung, C. S., Nam, S. Y. and Kang, C. Y. (1993b) Phytoplankton populations in the western Bransfield Strait and the southern Drake Passage, Antarctica. *Korean J. Polar Res.*, **4**, 29–43.

Kang, S.-H., Kim, D. Y., Kang, J. S., Lee, M. Y. and Lee, S. H. (1995) Antarctic phytoplankton in the eastern Bransfield region and in the northwestern Weddell Sea marginal ice zone during austral summer. *Korean J. Polar Res.*, **6**, 1–30.

Lancelot, C., Mathot, S., Veth, C. and Baar, H. de. (1993) Factors controlling phytoplankton ice-edge blooms in the marginal ice-zone of northwestern Weddell Sea during sea ice retreat 1988: field observations and mathematical modelling. *Polar Biol.*, **13**, 377–387.

Martin, J. H., Fitzwater, S. E. and Gordon, R. M. (1990) Iron deficiency limits phytoplankton growth in Antarctic waters. *Global Biogeochem. Cycles*, **4**, 5–12.

Mitchell, B. G. and Holm-Hansen, O. (1991) Observations and modelling of the Antarctic phytoplankton crop in relation to mixing depth. *Deep-Sea Res.*, **38**, 981–1007.

Park, M. K., Yang, S. R., Kang, S. H., Chung, K. H. and Shim, J. H. (1999) Phytoplankton biomass and primary production in the marginal ice zone of the northwestern Weddell Sea during austral summer. *Polar Biol.*, **21**, 251–261.

Parsons, T. R., Maita, Y. and Lalli, C. M. (1984) *A Manual of Chemical and Biological Methods for Seawater Analysis*. Pergamon Press, Toronto.

Pollard, R. T., Read, J. F., Allen, J. T., Griffiths, G. and Morrison, A. I. (1995) On the physical structure of a front in the Bellingshausen Sea. *Deep-Sea Res.*, **42**, 955–982.

Sakshaug, E. and Holm-Hansen, O. (1984) Factors governing pelagic production in polar oceans. In Holm-Hansen, O., Bolis, L. and Gilles, R. (eds), *Marine Phytoplankton and Productivity.* Springer-Verlag, Berlin, pp. 1–18.

Sakshaug, E., Slagstad, D. and Holm-Hansen, O. (1991) Factors controlling the development of phytoplankton blooms in the Antarctic Ocean—a mathematical model. *Mar. Chem.*, **35**, 259–271.

Schloss, I. and Estrada, M. (1994) Phytoplankton composition in the Weddell–Scotia Confluence area during austral spring in relation to hydrography. *Polar Biol.*, **14**, 77–90.

Smayda, T. J. (1978) From phytoplankton to biomass. In Sournia, A.

(ed.), *Monographs on Oceanic Methodology. 6. Phytoplankton Manual.* UNESCO, Paris, pp. 273–279.

Smetacek, V. and Passow, U. (1990) Spring bloom initiation and Sverdrup's critical depth model. *Limnol. Oceanogr.*, **23**, 1256–1263.

Smetacek, V., Scharek, R. and Nöthig, E. M. (1990) Seasonal and regional variation in the pelagial and its relationship to the life history cycle of krill. In Kerry, R. and Hempel, G. (eds), *Antarctic Ecosystems: Ecological Change and Conservations.* Springer-Verlag, Berlin, pp. 103–114.

Smith, W. O., Jr and Nelson, D. M. (1986) Importance of ice edge phytoplankton production in the Southern Ocean. *Biol. Sci.*, **36**, 251–257.

Smith, W. O., Jr and Nelson, D. M. (1990) Phytoplankton growth and new production in the Weddell Sea marginal ice zone in the austral spring and autumn. *Limnol. Oceanogr.*, **35**, 809–821.

Stammerjohn, S. E. and Smith, R. C. (1996) Spatial and temporal variability of western Antarctic Peninsula sea ice cover. In Ross, R. M., Hofmann, E. E. and Quetin, L. B. (eds), *Foundations for Ecological Research West of the Antarctic Peninsula. Antarctic Res. Ser.*, **70**, 81–104.

Sverdrup, H. U. (1953) On conditions for the vernal blooming of phytoplankton. *J. Cons. Int. Explor. Mer*, **18**, 287–295.

Veth, C., Lancelot, C. and Ober, S. (1992) On processes determining the vertical stability of surface waters in the marginal ice zone of the north-western Weddell Sea and their relationship with phytoplankton bloom development. *Polar Biol.*, **12**, 237–243.

Villafañe, V. E., Helbling, E. W. and Holm-Hansen, O. (1995) Spatial and temporal variability of phytoplankton biomass and taxonomic composition around Elephant Island, Antarctica, during the summers of 1990–1993. *Mar. Biol.*, **123**, 677–686.

Wilson, D. L., Smith, W. O., Jr and Nelson, D. M. (1986) Phytoplankton bloom dynamics of the western Ross Sea ice edge. I. Primary productivity and species-specific production. *Deep-Sea Res.*, **33**, 1375–1387.

Zwally, H. J., Comiso, J. C., Parkinson, C. L., Campbell, W. J., Carsey, F. D. and Gloersen, P. (1983) Antarctic Sea Ice, 1973–1976: Satellite passive-microwave observations, NASA SP-459. US Government Printing Office, Washington, DC, 206 pp.

Received on June 4, 2000; accepted on November 7, 2000